Ab Initio Study of the Spectroscopy of CH_3N and CH_3CH_2N

Chun-Yuan Hou, Hong-Xing Zhang,* and Chia-chung Sun

State Key Laboratory of Theoretical and Computational Chemistry, Institute of Theoretical Chemistry, Jilin University, Changchun 130023, People's Republic of China

Received: January 25, 2006; In Final Form: April 29, 2006

Complete active space (CAS) calculations with 6-311++g(3df,3pd) basis sets were performed for a large number of electronic states of the nitrate free radical (CH_3N/CH_3CH_2N) and their positive and negative ions. All calculated states are valence states, and their characters are discussed in detail. To investigate the Jahn−Teller effect on the CH_3N radical, C_s symmetry was used for both CH_3N and CH_3CH_2N in calculations. The results (CASPT2 adiabatic excitation energies and CASSI oscillator strengths) suggest that the calculated transitions of CH_3N at 32172 and 32139 cm^{-1} are attributed to the $2^3A'' \rightarrow 1^3A''$ and $1^3A' \rightarrow 1^3A''$, respectively, which is in accordance with the $\tilde{A}^3E \rightarrow \tilde{X}^3A_2$ emission spectrum at $T_0 = 31\,817$ cm^{-1}. The calculated transitions of CH_3CH_2N at 334 nm are attributed to the $1^3A'' \rightarrow 2^3A''$ and $1^3A'' \rightarrow 1^3A'$, respectively, which is in accordance with the UV absorption spectrum of a series of 11 bands beginning at 335 nm. The vertical and adiabatic ionization energies were obtained to compare with the PES data. These results are in agreement with previous experimental data, which is discussed in detail.

Introduction

Nitrate free radicals (molecules formulated as R−N) contain electron-deficient nitrogen atoms[1] and are extremely reactive species. As the simplest alkyl nitrene, CH_3N is a kind of dielectronic radical similar to carbene CH_2**:** and is thought to be an important intermediate in many organic and inorganic reactions.[2,3]

The first ab initio calculation of the different electronic states of CH_3N was reported in 1974 by Yarkony et al.[4] They confirmed that the lowest $^3A_2$, ^1E, and $^1A_1$ electronic states of CH_3N, arising from the same electron configuration $1\alpha_1^2 2\alpha_1^2 3\alpha_1^2 4\alpha_1^2 1e^4 5\alpha_1^2 2e^2$, are analogous to the known $^3\Sigma^-$, $^1\Delta$, and $^1\Sigma^-$ states from $1\sigma^2 2\sigma^2 3\sigma^2 1\pi^2$ of the diatomic NH. NH has been rather well characterized by spectroscopists,[5−7] and it has a stable triplet ground and excited state and stable singlet excited states.[6] Therefore, CH_3N should be at least a stable triplet radical. However, from the 1950s to 1970s, great efforts had been made to obtain optical spectra of CH_3N through the photolysis and pyrolysis of various precursors,[8] especially methyl azide CH_3N_3, but only the isomer, CH_2NH, a transient species as CH_3N, was observed, which is of interest in astrophysics and has been observed in dark interstellar dust clouds.[9]

The first report of the electronic emission spectrum of CH_3N originates from Carrick and Engelking's 1984 work using the complex eigenvalue Shroedinger equation (CESE) method of radical production for spectroscopy.[10] Their spectrum is much broader than subsequent jet-cooled emission spectra[11] but clearly shows an electronic transition assigned to $A^3E \rightarrow X^3A_2$, with $T_0 = 31\,811$ cm^{-1}. Since then, several other groups have observed the same emission band.[11,12] The structure of the CH_3N radical was first determined by high-resolution gas-phase emission spectroscopy of the transition.[13] After several years, Zhao et al. obtained experimentally the vibrationally resolved laser-induced fluorescence spectra of a system of radical and determined the excited-state vibrational frequencies.[14,15] Since the first ab initio calculation of the different electronic states of methylnitrene was reported in 1974 by Yarkony et al.,[4] many calculations on it have been reported.[16−18] In contrast to CH_3N, less is known about CH_3CH_2N, although a few experimental and theoretical studies have been reported.[19−21] However, there have not been thorough theoretical studies about the excitation spectroscopy of CH_3N or CH_3CH_2N.

Several studies by photoelectron spectroscopy (PES) were also carried out which were mainly concerned with the vertical ionization of different molecular orbitals of CH_3N and CH_3CH_2N.[22,23] Wang et al. reported four experimental energies in the low ionization energy region for CH_3N and CH_3CH_2N. They also performed some limited ab initio calculations of the vertical ionization energies according to C_{3v} symmetry and C_s symmetry from the Gaussian2 (G2) and density functional theory (DFT) methods to explain their findings for CH_3N and CH_3CH_2N, respectively. However, the structures and properties of the ground and excited states which would be of importance in their cations (CH_3N^+ and $CH_3CH_2N^+$) were not treated by them. Moreover, the ionization energies they calculated are vertical ionization energies which are not thought of for geometry relaxation, but the adiabatic energies which would be of important contribution to the ionization energies and to explain the characters of the electronic states were not calculated.

In 1999, Paul observed the PES of the CH_3N^- anion; they measured the electron affinity of methylnitrene to be 0.022 ± 0.009 eV, confirmed that the methylnitrene anion (CH_3N^-) is stable, and they measured the singlet/triplet splitting of methylnitrene to be 1.352 ± 0.011 eV.[24] However, there have not been experimental or theoretical reports on the characters of the ground and excited electronic states of CH_3N^- and $CH_3CH_2N^-$.

The aim of the present paper is to study and characterize a large number of electronic states of CH_3N and CH_3CH_2N and their positive and negative ions. CASSCF and CASPT2 methods have proved to be effective for theoretical studies of electronic

* To whom correspondence should be addressed. E-mail: zhanghx@mail.jlu.edu.cn.

10.1021/jp060528b CCC: $33.50
Published on Web 08/04/2006

spectra of molecules.[25,27] Equilibrium geometries, harmonic frequencies, adiabatic excitation energies, and oscillator strength for the low-lying states of neutral species and their positive and negative ions at the CASPT2//CASSCF level of theory, which give insight into the characteristics of the electronic states, were determined. Preliminary results are also obtained for the vertical and adiabatic ionization energies of different orbitals in C_s symmetry for CH_3N and CH_3CH_2N, and they are in agreement with experimental data.

Methodology

The active space for CASSCF calculations contains 12(11, 13) and 8(7, 9) electrons and consists of 11/12 molecular orbitals that are all valence orbitals for CH_3N and CH_3CH_2N and their ions, respectively. For CH_3N, the full-valence active space was used; for CH_3CH_2N, the CH_3 group is stable and the active space orbitals should be less than 12 orbitals to ensure the accuracy of the results, consisting of 8 electrons and 12 molecular orbitals is suitable for CH_3CH_2N in calculation.

The geometry of every state was optimized at the complete active space-self consistent field (CASSCF) level of theory. Multiconfigurational linear response (MCLR) was used to calculate the harmonic frequencies, and CASPT2 was used to calculate the dynamic correction.

For all of the calculations, extended basis sets were used which contain polarization and diffuse basis functions to give sufficient flexibility to describe a variety of different states. We used the basis sets, denoted 6-311++g(3df,3pd) basis, which were employed in a previous study[26] where it is described in detail for all of the calculations, which are explained in the following. Because the $d_{x2+y2+z2}$-type basis is treated as an s-type basis is the reason for excess electrons in the orbitals in the Mulliken population analysis in some cases. It gives the contraction scheme (12s,6p,3d,1f)/[5s,4p,3d,1f] for the N and C atoms and (6s,3p,1d)/[4s,3p,1d] for the H atom with a total of 135/207 contractions for CH_3N/CH_3CH_2N and their positive and negative ions.

To investigate the distortion of the excited states of CH_3N, we performed the geometry optimizations under C_s symmetry for every state of CH_3N and CH_3CH_2N at the CASSCF level. The oscillator strength is defined as

$$f = \frac{2}{3}(\mathrm{TDM})^2 \Delta E$$

The transition moments were computed by CASSCF, and the excitation energies which are very sensitive to dynamic correlation were computed by CASPT2.[27]

We used the optimized geometry of the ground state of CH_3N/CH_3CH_2N to calculate the vertical ionization energies which were obtained from the difference of the total energies between the resulting radical ion and the neutral CH_3N/CH_3CH_2N diradical. The calculated adiabatic ionization energies are obtained from the difference of the total energies between the radical ion and the neutral CH_3N/CH_3CH_2N diradical under their respective optimized geometry. All of the calculations were performed using the MOLCAS 5.4 quantum-chemistry software[28] on a Lenovo/1800 server.

Results and Discussion

A. Adiabatic and Vertical Excitation Energies and State Characteristics of CH_3N and CH_3CH_2N. The calculation of the excitation spectrum is a natural starting point for a thorough investigation of the excited states of any polyatomic system. A few electronic states by the CASSCF method, which provides us with dipole transition moments for the calculation of oscillator strengths, were calculated. Furthermore, the configuration interaction (CI) vectors of the CASSCF wave function give insight into the structure of the respective electronic state and will be discussed in the following. For all of the calculated states, we improved the accuracy of the adiabatic excitation energies by including dynamic electron correlation by the CASPT2 method.

1. CASPT2//CASSCF Results for the Ground and Excited States of CH_3N and CH_3CH_2N. We optimized equilibrium structures of the ground states and 7/8 lowest excited states of CH_3N/CH_3CH_2N by CASSCF to obtain good starting guesses and approximate Hessians for the computationally extremely demanding CI optimizations. All of the states for the experimental C_s equilibrium geometry that we obtained at the CASPT2//CASSCF level are summarized in Table 1a and Table 2a, which contain energies and oscillator strengths. We will first describe the results of CH_3N and then compare the results of CH_3CH_2N with them.

Hyperconjugation arguments are often evoked when discussing the bonding in open-shell systems, usually in the context of explaining ESR or PES data. In our calculations, we find that the effect of C−N hyperconjugation would shorten the N−C bond length as shown in Figure 2c (Supporting Information). Moreover, increased s character along the C−N axis, characteristic of a strong σ-type N−C bond, enhances the C−N bond since excess electrons occupied the stabilized N−C σ-type bond and are at the expense of s character in the C−H bonds, which results in carbon p-type orbitals that play a more important role in the C−H bonds. Thus, it weakened C−H bonds and made the HCH bond angle tend to 90°, exactly as found in the optimized ground geometry, as determined by Chappell and Engelking.[11] In the $2^3A''$ and $1^3A'$ excited states, the σ-type N−C bond is weakened because of an electron transfer from the C−N σ-type bond to the HOMO(2e) orbital, and the C−H bonds are strengthened, thus the C−N bond is lengthened, the HCH bond angle is a little bigger, and the NCH bond angle is a little smaller.

The Jahn−Teller effect is not evident in the ground state, since it retains C_{3v} symmetry. We find in excited states the geometry was also affected little as is found throughout Table 1a. The $^1A'$, $^3A'$, and $2^1A''$ states have one short and two long C−H bonds, and the $^1A''$, $2^3A''$, and $3^1A'$ states distort from C_{3v} symmetry in the opposite sense. However, the distortion from C_{3v} symmetry of both components of ^1E and ^3E is quite small; the $^1A'$ and $^1A''$ states, $^3A'$ and $2^3A''$ states, and $2^1A''$ and $3^1A'$ states differ in energy by less than 0.01 eV. The C−N bond length in the $^1A'$ and $^1A''$ states is nearly the same, and both are slightly shorter than the C−N bond length in the $^3A''$ state as found by Borden et al.[29] The C−N bond lengths in the $^3A'$ and $2^3A''$ states are slightly longer than the C−N bond length in the $^3A''$ state, and the C−N bond ruptures in the $2^1A''$ and $3^1A'$ states.

The oscillator strengths for the transitions between the ground and excited states were calculated. To obtain a nonvanishing transition dipole moment, $\langle \psi_i | \hat{\mu} | \psi_j \rangle$, the direct product, $\Gamma_i \times \Gamma_\mu \times \Gamma_j$, must contain the totally symmetric irreducible representation. In the case of the C_s point group, $\Gamma_{\mu y}$ and $\Gamma_{\mu z}$ are A′ and the ground-state symmetry is $1^3A''$, thus transitions into states of A″ symmetry are dipole allowed, and $\Gamma_{\mu x}$ is A″, thus transitions into states of A′ symmetry are dipole allowed.

TABLE 1:

(a) Total Energies, Adiabatic Excitation Energies, Oscillator Strengths, and Optimized Structures of Ground and Excited States of CH_3N as Calculated by CASPT2//CASSCF

state	R1[a] (Å)	R2[a] (Å)	R3[a] (Å)	α1[b] (deg)	α2[b] (deg)	α3[b] (deg)	α4[b] (deg)	CASSCF E (au)	CASPT2 E (au)	E_v (cm^{-1})	f
$^3A''$	1.446	1.110	1.110	110.6	110.6	108.4	108.4	−94.123867	−94.410685		
exp[c]	1.411	1.09				106.68					
$^1A'$	1.417	1.112	1.118	112.3	110.7	107.9	107.2	−94.058218	−94.357749	11617	$<10^{-10}$
$^1A''$	1.417	1.119	1.114	110.8	111.4	107.7	107.8	−94.058208	−94.357805	11604	$<10^{-10}$
$2^1A'$	1.414	1.117	1.117	111.3	111.3	107.6	107.5	−94.026794	−94.322790	19288	$<10^{-10}$
$^3A'$	1.509	1.102	1.105	104.3	109.9	110.6	111.3	−93.972327	−94.264230	32139	0.225
$2^3A''$	1.510	1.106	1.103	111.1	106.5	111.1	110.3	−93.972214	−94.264081	32172	1.773
$3^1A'$	1.701	1.097	1.096			114.8	115.7	−93.925936	−94.210400	43952	$<10^{-10}$
$2^1A''$	1.702	1.096	1.096			115.5	114.4	−93.925907	−94.210368	43959	$<10^{-10}$

(b) Leading Configurations, Occupation, and Respective Weights in the CI Vector (c^2) of CH_3N Electronic States from CASSCF Calculations

sym.	occupation[d]	weight	sym.	occupation[d]	weight
$^3A''$	22220u00 2u0	0.936	$3^1A'$	222u0d00 220	0.937
$^1A'$	22220200 200	0.505	$2^3A''$	222u0200 2u0	0.935
	22220000 220	0.439	$^3A'$	222u0u00 220	0.935
$^1A''$	22220u00 2d0	0.944	$2^1A''$	222u0200 2d0	0.938
$2^1A'$	22220200 200	0.457			
	22220000 220	0.458			

(c) Harmonic Frequencies of Ground and Excited States of CH_3N as Calculated by MCLR

state	υ_1''[e]	υ_2''[e]	υ_3''[e]	υ_4''[e]	υ_5''[e]	υ_6''[e]
$^3A''$	2854	1403	1009	2923	1469	999
exp[f]	2943	1349	1040	2989	1490	903
$^3A'$	2891	1393	750	3016/2971	1502/1450	809/1072
exp[g]			759	2943	1500	
$2^3A''$	2889	1397	810	2982/3017	1463/1497	1183/i808
$^1A'$	2894	1379	1043	2782/2394	1421/1428	558/972
$^1A''$	2850	1372	1044	2769/1908	1416/1412	969/i1187
$2^1A'$	2797	1369	1069	2859/2859	1438/1438	1145/1143
$3^1A'$	2965	1263	879	3114/3109	1424/1460	507/472
$2^1A''$	2967	1269	914	3115/3107	1447/1447	507/i430

[a] R1 is the N−C distance, R2 is the C−H1 distance, and R3 is the C−H2 distance. [b] α1 is the N−C−H1 angle, α2 is the N C H2 angle, α3 is the H1 C H2 angle, and α4 is the H2−C−H2(X) angle. The geometry of CH_3N is restricted to C_s symmetry. All states were optimized at the CASPT2/CASSCF level using 6-311++g(3df,3pd) basis sets. [c] Carrick, P. G.; Brazier, C. R.; Bernath, P. F.; Engelking, P. C. ref 13. [d] The occupation number represents the electronic number that is occupied in the active space. u represents a spin-up electron, and d represents a spin-down electron. [e] υ_1'' represents the symmetric hydrogen stretch, υ_2'' represents the symmetric hydrogen bend, υ_3'' represents the C−N stretch, υ_4'' represents the asymmetric hydrogen stretch, υ_5'' represents the scissors, and υ_6'' represents the rock. [f] Chappell, E. L.; Engelking, P. C., ref 11. [g] Zhao, X.; et al., ref 14.

TABLE 2:

(a) Optimized Geometries, Excited Energies, and Oscillator Strengths of the CH_3CH_2N Radical

state	R1[a] (Å)	R2[a] (Å)	R3[a] (Å)	R4[a] (Å)	R5[a] (Å)	α1[b] (deg)	α2[b] (deg)	α3[b] (deg)	α4[b] (deg)	α5[b] (deg)	α6[b] (deg)	α7[b] (deg)	α8[b] (deg)	CASSCF E (au)	CASPT2 E (au)	T_v (nm)	f
$^3A''$	1.433	1.557	1.086	1.082	1.104	108.9	110.9	109.9	108.0	110.7	109.4	108.9	108.5	−133.165206	−133.649713		
$2^3A''$	1.612	1.499	1.076	1.079	1.111			114.6	111.2	111.3	107.8	109.4	108.5	−133.054098	−133.513120	334	0.057
$^3A'$	1.614	1.499	1.076	1.079	1.108			114.0	112.3	111.4	107.5	109.8	108.4	−133.053757	−133.512020	334	0.004
$^1A'$	1.413	1.554	1.090	1.082	1.105	106.9	115.1	110.8	105.8	110.5	109.8	108.8	108.6	−133.112272	−133.592933	802	$<10^{-10}$
$^1A''$	1.413	1.566	1.087	1.081	1.104	109.4	110.9	109.5	108.1	110.6	108.9	109.2	108.8	−133.110044	−133.596373	854	$<10^{-10}$
$2^1A'$	1.449	1.527	1.088	1.082	1.105	108.1	111.6	110.7	107.5	110.9	109.6	108.7	108.3	−133.090364	−133.561227	515	$<10^{-10}$
$3^1A'$	1.781	1.489	1.073	1.079	1.110			116.7	114.8	111.5	107.2	110.0	108.2	−133.012599	−133.464765	246	$<10^{-10}$
$2^1A''$	1.768	1.488	1.073	1.079	1.112			116.7	114.8	111.5	107.2	110.0	108.2	−133.012599	−133.464765	246	$<10^{-10}$
$4^1A'$	2.183	1.469	1.072	1.077	1.100			121.1	117.4	111.5	102.6	112.4	109.1	−132.897258	−133.327859	142	$<10^{-10}$

(b) Leading Configurations, Occupation and Respective Weights in the CI Vector (c^2) of CH_3CH_2N Electronic States from CASSCF Calculations

sym.	occupation[c]	weight	sym.	occupation[c]	weight
$^3A''$	222u00000 u00	0.944	$2^1A'$	222200000 000	0.459
$2^3A''$	22u200000 u00	0.926		222000000 200	0.455
$^3A'$	22uu00000 200	0.926	$3^1A'$	22ud00000 200	0.926
$^1A'$	222200000 000	0.721	$2^1A'$	22u200000 d00	0.929
	222000000 200	0.222	$4^1A'$	220200000 200	0.851
$^1A''$	222u00000 d00	0.945			

[a] R1 is the N1−C1 distance, R2 is the C1−C2 distance, R3 is the C1−H1 distance, R4 is the C2−H2 distance, and R5 is the C2−H3 distance. [b] α1 is the N1−C1−H1 angle, α2 is the N1−C1−C2 angle, α3 is the C2−C1−H1 angle, α4 is the H1−C1−H1(Z) angle, α5 is the C1−C2−H2 angle, α6 is the C1−C2−H3 angle, α7 is the H2−C2−H2(Z) angle, and α8 is the H2−C2−H3 angle. The geometries were restricted to C_s symmetry and optimized at the CASPT2//CASSCF level of theory using 6-311++g(3df,3pd) basis sets. [c] The occupation number represents the electronic number that is occupied in the active space. u represents a spin-up electron, and d represents a spin-down electron.

Our calculated oscillator strengths (cf. Table 1a) reflect exactly these selection rules, and within numerical accuracy, oscillator strengths of transitions into states $^1A'$ and $^1A''$ are above 10 orders of magnitude smaller than those for $1^3A'$ and $2^3A''$. It also shows that transitions from the triplet state into triplet states are available.

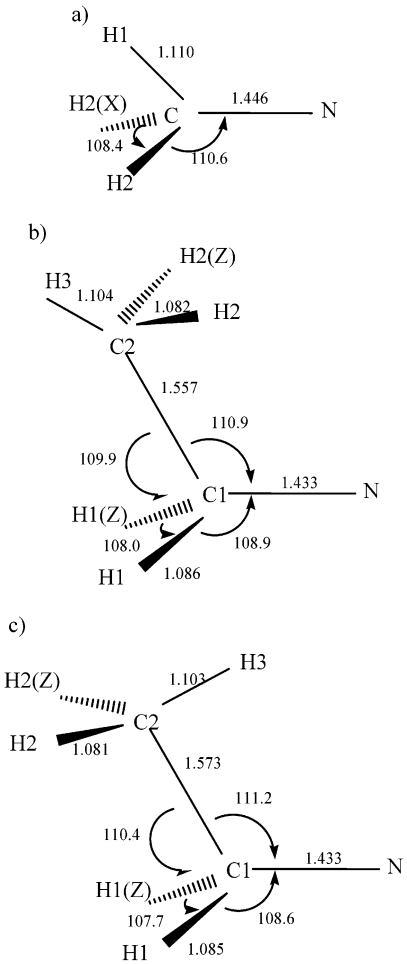

Figure 1. Optimized structure of the $^3A''$ state of (a) CH_3N and (b) CH_3CH_2N at cross configuration and (c) CH_3CH_2N at parallel configuration using CASSCF calculations.

Supporting Information Table 9a gives the Mulliken population analysis for the $^3A''$ ground state and $1^3A'$ and $2^3A''$ excited states. We can see that only the population on the C and N atoms is different. In the ground state, the electronic configuration of the C/N atoms is $s^{2.979}p_x^{0.954}p_y^{0.954}p_z^{0.627}/s^{4.109}p_x^{1.034}p_y^{1.034}p_z^{1.268}$, while in the $2^3A''$ and $1^3A'$ excited states the configurations are $s^{3.013}p_x^{0.976}p_y^{0.956}p_z^{0.453}/s^{3.889}p_x^{1.015}p_y^{1.961}p_z^{0.699}$ and $s^{3.012}p_x^{0.958}p_y^{0.972}p_z^{0.453}/s^{3.889}p_x^{1.962}p_y^{1.016}p_z^{0.698}$, respectively. The $2^3A'' \rightarrow 1^3A''$ transition calculated at 32 172 cm^{-1} has the largest oscillator strength of 1.773, but the calculated frequency values of the $2^3A''$ state show a negative value which indicates CH_3N is not stable in the $2^3A''$ state, and the $1^3A' \rightarrow 1^3A''$ transition calculated at 32 139 cm^{-1} has an oscillator strength of 0.225, thus we relate the two transitions to the experimental $\tilde{A}^3E \rightarrow \tilde{X}^3A_2$ emission spectra at $T_0 = 31\,817$ cm^{-1}.[10-12] In the transitions, about 0.93 P_x or P_y electron on the N atom is transferred to the s and p orbitals of the C and N atoms at a ratio 1:4 statistically. We assigned it to be $(ps)_H \rightarrow (sp)_\sigma$ in nature, and the two orbitals are shown in parts a and b of Supporting Information Figure 2. We can also see that in the $^2A'$ state of CH_3N^+ or in the $^2A'$ and $^2A''$ states of CH_3N^- an electron dominantly moves away or in the $(ps)_H$ orbital. The evident change of population of s orbitals on H atoms is greater than that in the $2^3A''$ and $1^3A'$ excited states of CH_3N and is the reason for the shorter C−N bond length which strengthens the N−H interaction. We can see analogous results for CH_3CH_2N in Table 9b (Supporting Information), however, the effect of hyperconjugation is less than that in CH_3N and the orbital character is a little different in the $2^3A''$ and $1^3A'$ excited states of CH_3CH_2N. Except for the two excited states of $1^1A'$ and $1^1A''$ at excitation energies of 11 608 and 11 609 cm^{-1}, respectively, excitation energies are all above the photodissociation limit of 17 000 to 18 000 cm^{-1}. However, there have not been experimental reports on the $2^1A'$, $3^1A'$, or $2^1A''$ states, perhaps modern spectroscopic methods would be capable of observing these states which might be an interesting challenge for experimentalists. The CASPT2//CASSCF adiabatic excitation energies (T_0) and state properties yield a picture of the electronic spectrum of CH_3N, including several states never calculated nor measured before. We calculated the triplet/singlet splitting energies to be 1.439 eV which is compared with the experimental 1.352 eV data.[24]

The results of CH_3CH_2N are summarized in Table 2a. The two isomers energies demonstrate that the cross configuration is a little more stable. By comparing the results of CH_3N with CH_3N, we find: (1) The effect of hyperconjugation is weakened by replacing a H atom with a CH_3 group. (2) The adiabatic excitation energies at 334 nm compared with the UV absorption spectrum in solid nitrogen consist of a series of 11 bands beginning at 335 nm[1].[9] The red shift is the reason for the CH_3 group which delocates the electron between the N and C atoms (cf. Table 9b, Supporting Information). The vertical transition energies are also obtained for CH_3N and CH_3N (cf. Table 8). (3) In the ground state, the N−C distance of CH_3CH_2N is shorter than that of CH_3N and the N−C bonding of CH_3CH_2N is stronger than that of CH_3N. In the $^3A'$ and $2^3A''$ excited states, the N−C bond is ruptured in CH_3CH_2N and weakened in CH_3N. (4) The triplet/singlet splitting energy of CH_3CH_2N is 1.451 eV.

2. Characteristics of Electronic States. With the CASSCF framework, each state is characterized by its CI vector which in general is easily interpreted. Most states can be well described by one dominant electron configuration which reveals the excitation process by which the respective state arises from the electronic ground states. In Tables 1b and 2b, we compile the leading electron configuration, the occupation in which u represents an electron spin orientation that is "up" and d represents one that is "down", and their respective weights (c^2) in the CASSCF wave function for all calculated states. The CH_3N ground state retains C_{3v} symmetry and is dominantly $(3a')^2(4a')^2(5a')^2(1a'')^2(6a')^2(8a')^1(2a'')^1$, in which the 6a′ and 1a″ orbitals are degenerate orbitals and the 8a′ and 2a″ orbitals are degenerate orbitals as is shown in parts a and c of Supporting Information Figure 2 and it is in accordance with the 1e and 2e orbitals in C_{3v} symmetry. The CH_3CH_2N ground state is dominantly $(7a')^2(8a')^2(9a')^2(3a'')^1(10a')$.[1] In the CH_3N ground state, the two unpaired electrons reside in the 8a′ and 2a″ molecular orbitals which are perpendicular to the N−C bond and are mostly composed of the $2p_y$ and the $2p_x$ orbitals of the N atom and show a small degree of the N−H interaction character. States 3 and 4 mainly result from single excitations between the two degenerate orbitals.

In fact, the majority of the calculated states arise from single or double excitations into the two orbitals which are the energetically lowest, not completely occupied, orbitals in the ground state. In the ground state of CH_3CH_2N, the two unpaired electrons reside in the 15a′ and 3a″ orbitals between which the calculated orbital energy interval is very small.

The c^2 values of all of the states leading configurations are above 0.9, indicating a single-reference character of the respective states except the $^1A'$ and $2^1A'$ states of CH_3N and CH_3CH_2N, which also reflect that the 8a′ and 2a″ orbitals of CH_3N

TABLE 3:

(a) Total Energies, Adiabatic Excitation Energies, Oscillator Strengths, and Optimized Structures of Ground and Excited States of CH_3N^+ as calculated by CASSCF

state	R1[a] (Å)	R2[a] (Å)	R3[a] (Å)	α1[b] (deg)	α2[b] (deg)	α3[b] (deg)	α4[b] (deg)	α5[b] (deg)	CASSCF *E* (au)	CASPT2 *E* (au)	T_v (nm)	*f*
$^2A'$	1.317	1.109	1.158	121.2	103.9	116.9	88.4		−93.766200	−94.020970		
$^4A''$	1.644	1.100	1.100			116.5	116.5		−93.736199	−93.975214	996	$<10^{-10}$
$^4A'$	1.486	1.077	1.211	121.3	117.2	112.8	60.6	59.7	−93.640397	−93.901780	382	$<10^{-10}$
$2^2A''$	1.775	1.100	1.100			118.1	118.2		−93.657312	−93.895364	363	0.001
$2^2A'$	1.717	1.102	1.102			118.0	117.7		−93.626489	−93.884344	334	0.164
$3^2A'$	1.732	1.104	1.104			118.2	118.2		−93.588309	−93.838336	249	0.008

(b) Leading Configurations, Occupation, and Respective Weights in the CI Vector (c^2) of CH_3N^+ Electronic States from CASSCF Calculations

sym.	occupation[c]	weight	sym.	occupation[c]	weight	sym.	occupation[c]	weight
$^2A'$	2222u000 200	0.912	$2^2A''$	222ud000 2u0	0.701	0.234	222u0000 220	0.471
$^4A''$	222uu000 2u0	0.918		222uu000 2d0	0.234	$3^2A'$	222u2000 200	0.459
$^4A'$	2222u000 uu0	0.941	$2^2A'$	222u2000 200	0.473	0.471	222u0000 220	0.459

[a] R1 is N−C the distance, R2 is the C−H1 distance, and R3 is the C−H2 distance. [b] α1 is the N−C−H1 angle, α2 is the N−C−H2 angle, α3 is the H1−C−H2 angle, α4 the H2−C−H2(X) angle, and α5 is the C−H2−H2(X) angle. The geometry of CH_3N^+ is restricted to C_s symmetry. All states were optimized at the CASPT2//CASSCF level using 6-311++g(3df,3pd) basis sets. [c] The occupation number represents the electronic number that is occupied in the active space. u represents a spin-up electron, and d represents a spin-down electron.

TABLE 4:

(a) Optimized Geometries and Total Energies of $CH_3CH_2N^+$ Radical Electronic States

state	R1[a] (Å)	R2[a] (Å)	R3[a] (Å)	R4[a] (Å)	R5[a] (Å)	α1[b] (deg)	α2[b] (deg)	α3[b] (deg)	α4[b] (deg)	α5[b] (deg)	α6[b] (deg)	α7[b] (deg)	α8[b] (deg)	CASSCF *E* (au)	CASPT2 *E* (au)
$^2A'$	1.325	1.564	1.115	1.079	1.100	101.2	118.5	116.5	99.9	109.9	106.7	110.8	109.7	−132.793668	−133.267129
$^4A'$	1.484	1.989	1.078	1.076	1.075	114.9		122.5				118.3	118.2	−132.624496	−133.040094

(b) Leading Configurations, Occupation, and Respective Weights in the CI Vector (c^2) of $CH_3CH_2N^+$ Electronic States from CASSCF Calculations

sym.	occupation[c]	weight
$^2A'$	222u00000 000	0.934
$^4A'$	uu2u00000 200	0.938

[a] R1 is the N1−C1 distance, R2 is the C1−C2 distance, R3 is the C1−H1 distance, R4 is the C2−H2 distance, and R5 is the C2−H3 distance. [b] α1 is the N1−C1−H1 angle, α2 is the N1−C1−C2 angle, α3 is the C2−C1−H1 angle, α4 is the H1−C1−H1(Z) angle, α5 is the C1−C2−H2 angle, α6 is the C1−C2−H3 angle, α7 is the H2−C2−H2(Z) angle, and α8 is the H2−C2−H3 angle. The geometries were restricted to C_s symmetry and optimized at the CASPT2//CASSCF level of theory using 6-311++g(3df,3pd) basis sets. [c] The occupation number represents the electronic number that is occupied in the active space. u represents a spin-up electron and d represents a spin-down electron.

in the $^1A'$ and $2^1A'$ states are degenerate orbitals and the $4^1A'$ state of CH_3CH_2N which indicates a low multireference character. We can predict that in high excited states it will show high multireference character.

3. Harmonic Frequencies. The experimental frequency values for all the vibrational modes in the ground state of CH_3N were reported in several papers.[10−13] The frequency values of CH_3N which are summarized in Table 1c at the CASSCF level using the MCLR program of the MOLCAS 5.4 software were calculated. The calculated υ_2'' and υ_6'' values in the $1^3A''$ state are slightly bigger than the experimental values in the 1^3A_2 ground state. The calculated υ_1'', υ_3'', υ_4'', and υ_5'' values are slightly smaller than the experimental values in the 1^3A_2 ground state. The calculated υ_3'' values in the $1^1A''$, $1^1A'$, and $2^1A'$ excited states are bigger than that in the $1^3A''$ state as the C−N bond length is shorter, which is in accordance with Zhao et al.'s work.[15] The calculated υ_3'' values in the $2^3A''$, $^3A'$, $3^1A'$, and $2^1A''$ excited states are smaller than that in the $1^3A''$ state as the C−N bond length is longer.

B. Excitation and Ionization Energies and State Characteristics of CH_3N^+ and $CH_3CH_2N^+$. To further investigate the chemical properties of CH_3N and CH_3CH_2N, the ground and excited states of CH_3N^+ and $CH_3CH_2N^+$ using the same basis sets and methods as the neutral molecules were calculated. All of the states for the experimental C_s equilibrium geometry that we obtained at the CASPT2//CASSCF level are summarized in Table 3a and Table 4a, which contain energies and oscillator strengths. Furthermore, the vertical ionization energies which are obtained from the difference of the total energies between the resulting radical ion and the neutral CH_3N/CH_3CH_2N diradical were calculated. The calculated adiabatic ionization energies are obtained from the difference of the total energies between the radical ion and the neutral CH_3N/CH_3CH_2N diradical under their respective optimized geometry.

1. CASPT2//CASSCF Results for the Ground and Excited States of CH_3N^+ and $CH_3CH_2N^+$. Their adiabatic excitation energies, which had never been reported and the results were summarized in Table 3a and Table 4a, were calculated. The CASSCF calculations are not appropriate for a theoretical study of the $1^2A''$ state of CH_3N^+ or $CH_3CH_2N^+$ because there is no energy minimum unless it undergoes a pathway into their amine cations. However, even though the state exists, it is not the ground state of CH_3N^+ because the $1^2A'$ and $1^2A''$ states in the ground state of CH_3N^+ in $C_{3\upsilon}$ symmetry split due to the Jahn−Teller effect and the $1^2A'$ state energy is lower than that in $C_{3\upsilon}$ symmetry. So, the $1^2A'$ state is the ground state in our calculation of CH_3N^+ and $CH_3CH_2N^+$. We predict a strong transition in the adiabatic excitation spectrum of CH_3N^+ at $\lambda = 334$ nm and a weak transition at $\lambda = 249$ nm.

The c^2 values of the $^2A'$, $^4A''$, and $^4A'$ states leading configurations of CH_3N^+ are above 0.9, indicating a single-reference character of the respective states. In the $2^2A''$, $2^2A'$,

TABLE 5:

(a) Total Energies, Adiabatic Excitation Energies, Oscillator Strengths, and Optimized Structures of Ground and Excited States of CH_3N^- as Calculated by CASSCF

state	R1[a] (Å)	R2[a] (Å)	R3[a] (Å)	α1[b] (deg)	α2[b] (deg)	α3[b] (deg)	α4[b] (deg)	CASSCF *E* (au)	CASPT2 *E* (au)	E_v (nm)	*f*
$^2A'$	1.412	1.134	1.156	110.3	118.2	102.9	102.2	−94.060378	−94.398542		
$^2A''$	1.412	1.168	1.139	119.9	113.5	102.4	103.2	−94.060199	−94.398272		
$^4A''$	1.447	1.082	1.109	111.4	110.9	108.2	106.9	−94.059543	−94.375795	2003	$<10^{-10}$
$^4A'$	1.449	1.114	1.090	108.6	109.97	107.32	113.5	−94.024492	−94.344352	841	$<10^{-10}$
$2^2A''$	1.427	1.086	1.093	110.9	111.9	108.0	105.8	−93.991760	−94.319909	582	0.001
$2^4A''$	1.534	1.098	1.098	110.3	106.5	111.5	110.3	−93.909581	−94.231477	273	$<10^{-10}$
$2^4A'$	1.552	1.105	1.076	108.9	105.0	111.2	115.0	−93.881943	−94.197349	226	$<10^{-10}$
$3^4A'$	1.401	1.209	1.209	126.5	126.	88.3	88.3	−93.773804	−94.121232	164	$<10^{-10}$

(b) Leading Configurations, Occupation, and Respective Weights in the CI Vector (c^2) of CH_3N^- Electronic States from CASSCF Calculations

sym.	occupation[c]	weight	sym.	occupation[c]	weight	sym.	occupation[c]	weight
$^2A'$	22220u00 220	0.939	$2^2A''$	2222ud00 2u0	0.239	$2^4A'$	222u2000 2uu	0.945
$^2A''$	22222000 2u0	0.939		2222uu00 2d0	0.722	$3^4A'$	22222u00 uu0	0.474
$^4A''$	2222uu00 2u0	0.948	$2^4A''$	222u2u00 2u0	0.954		22u2uu00 220	0.474
$^4A'$	2222u000 2uu	0.952						

[a] R1 is the N−C distance, R2 is the C−H1 distance, and R3 is the C−H2 distance. [b] α1 is the N−C−H1 angle, α2 is the N−C−H2 angle, α3 is the H1−C−H2, and α4 is the H2−C−H2(X) angle. The geometry of CH_3N^- is restricted to C_s symmetry. All states were optimized at the CASPT2//CASSCF level using 6-311++g (3df,3pd) basis sets. [c] The occupation number represents the electronic number that is occupied in the active space. u represents a spin-up electron and d represents a spin-down electron.

TABLE 6:

(a) Optimized Geometries and Total Energies of the $CH_3CH_2N^-$ Radical

state	R1[a] (Å)	R2[a] (Å)	R3[a] (Å)	R4[a] (Å)	R5[a] (Å)	α1[b] (deg)	α2[b] (deg)	α3[b] (deg)	α4[b] (deg)	α5[b] (deg)	α6[b] (deg)	α7[b] (deg)	α8[b] (deg)	CASSCF *E* (au)	CASPT2 *E* (au)
$^4A''$	1.434	1.554	1.084	1.082	1.101	109.3	111.7	109.6	107.1	111.2	108.7	109.4	108.2	−133.114746	−133.618884
$^4A'$	1.431	1.554	1.086	1.082	1.105	108.7	110.8	109.1	110.3	110.5	108.9	110.4	108.2	−133.096950	−133.595373
$2^4A''$	1.659	1.490	1.073	1.079	1.108			115.3	111.2	111.8	106.6	110.4	108.0	−133.003945	−133.483355
$2^4A''$	1.635	1.494	1.076	1.079	1.112			113.8	114.1	111.3	107.0	110.8	108.0	−132.981903	−133.459263

(b) Leading Configurations, Occupation, and Respective Weights in the CI Vector (c^2) of $CH_3CH_2N^-$ Electronic States from CASSCF Calculations

sym.	occupation[c]	weight
$^4A''$	222uu0000 0u0	0.951
$^4A'$	22200u000 uu0	0.944
$2^4A''$	22u20u000 0u0	0.929
$2^4A'$	22u200000 0uu	0.929

[a] R1 is the N1−C1 distance, R2 is the C1−C2 distance, R3 is the C1−H1 distance, R4 is the C2−H2 distance, and R5 is the C2−H3 distance. [b] α1 is the N1−C1−H1 angle, α2 is the N1−C1−C2 angle, α3 is the C2−C1−H1 angle, α4 is the H1−C1−H1(Z) angle, α5 is the C1−C2−H2 angle, α6 is the C1−C2−H3 angle, α7 is the H2−C2−H2(Z) angle, and α8 is the H2−C2−H3 angle. The geometries were restricted to C_s symmetry and optimized at the CASPT2//CASSCF level of theory using 6-311++g(3df,3pd) basis sets. [c] The occupation number represents the electronic number that is occupied in the active space. u represents a spin-up electron and d represents a spin-down electron.

and $3^2A'$ excited states, the N−C bond ruptures and the c^2 values of these states indicate a multireference character, which shows that the 8a′ and 2a″ CH_3N^+ orbitals in these states are degenerate orbitals (cf. Table 3b and Table 4b).

2. Ionization Energies. There have been some photoelectron spectrum experimental and calculation reports about CH_3N and CH_3CH_2N,[22,23] however, their calculations were only emphasized on the vertical ionization energies. We calculated the adiabatic ionization energies and vertical ionization energies which were summarized in parts a and b of Table 7 and that further proved our findings. The difference between the vertical and adiabatic ionization energies of CH_3N is 0.34 eV. This means that the HOMO(2e) of the CH_3N diradical is not nonbonding orbitals but with a small degree of N−H interaction character, as described above.

3. Distortion from C_{3v} Symmetry. From the optimized geometries under C_s symmetry, we can see that the distortion from C_{3v} symmetry was evident in the $^2A'$ and $^4A'$ states, and in the $^4A'$ state of CH_3N^+, the two symmetric H atoms are bonding.

C. Excitation Energies and State Characteristics of CH_3N^- and $CH_3CH_2N^-$. To further investigate the chemical properties of CH_3N and CH_3CH_2N, the ground and excited states of CH_3N^- and $CH_3CH_2N^-$ using the same basis sets and methods were also calculated. All of the states for the experimental C_s equilibrium geometry that we obtained at the CASPT2//CASSCF level are summarized in Table 5a and Table 6a, which contain energies and oscillator strengths. Furthermore, we calculated the vertical electron affinity energy which is obtained from the difference of the total energies between the resulting radical ion and the neutral CH_3N/CH_3CH_2N radical. The calculated adiabatic electron affinity energy is obtained from the difference of the total energies between the radical ion and the neutral CH_3N/CH_3CH_2N radical under their respective optimized geometry.

1. CASPT2//CASSCF Results for the Ground and Excited States of CH_3N^- and $CH_3CH_2N^-$. The adiabatic excitation energies, which had never been reported and the results were summarized in Tables 5 and 6, were calculated. The CASSCF calculations are not appropriate for a theoretical study of the $1^2A''$ and $1^2A'$ states of $CH_3CH_2N^-$ because the states are repulsive. We predict a weak transition in the adiabatic excitation spectrum of CH_3N^- at $\lambda = 582$ nm.

TABLE 7:

(a) Calculated Vertical Ionization Energies (E_v), Adiabatic Ionization Energies (E_a), and $\Delta E(E_v - E_a)$ of CH_3N According to C_{3v} Symmetry from the CASPT2//CASSCF Method

cationic states	associated orbitals	E_v (ev)	E_a (ev)	ΔE (cm^{-1})	exp[a]
$^2A'$	2a″	11.17	10.60	4597	11.04
$^2A''$	7a′	11.17			11.04
$^4A''$	6a′	12.07	11.85	1774	11.40(12.85)
$^4A'$	1a″	15.17	13.85	10646	15.53

(b) Calculated Vertical Ionization Energies (E_v) and Adiabatic Ionization Energies (E_a) of CH_3CH_2N According to C_s Symmetry from the CASPT2//CASSCF Method

cationic states	associated orbitals	E_v (ev)	E_a (ev)	ΔE (cm^{-1})	exp[b]
$^2A'$	3a″	10.43	10.29	1129	10.19
$^2A''$	10a′	10.92			10.48
$^4A''$	9a′	11.59			12.06
$^4A'$	9a″	13.89	16.59	21774	13.89

[a] Jing, W.; Zheng, S.; Xinjiang, Z.; Xiaojun, Y.; Maofa, G.; Dianxun, W., ref 22. [b] Yang, X.; Zheng, S.; Maofa, G.; Zheng, S.; Meng, L.; Wang, D., ref 23.

TABLE 8: Vertical Excitation Energies (T_v, in nanometers) for Low-lying Excited Electronic States of CH_3N and CH_3CH_2N Obtained in the CASPT2 Calculations with 6-311++G(3df,3pd) Basis Sets

	absorption (T_v)		emission (T_v)	
	$1^3A'' \rightarrow 1^3A'$	$1^3A'' \rightarrow 2^3A''$	$1^3A'' \leftarrow 1^3A'$	$1^3A'' \leftarrow 2^3A''$
CH_3N	307	303	319	319
exp[a,b]	316		314	
CH_3CH_2N	323	326	368	372
exp[c]	335			

[a] Chappell, E. L.; Engelking, P. C., ref 11. [b] Ferrante, R. F., ref 12. [c] Ferrante, R. F.; Erickson, S. L.; Peek, B. M., ref 19.

The c^2 values of all the states leading configurations are above 0.9, indicating a single-reference character of the respective states, except for the $2^2A''$ state of CH_3N^- which shows that the 8a′ and 2a″ orbitals in the state are degenerate orbitals and the $3^4A'$ state of CH_3N^- which shows that the 6a′ and 1a″ orbitals in the state are also degenerate orbitals (cf. Table 5b and Table 6b). It is in accordance with the ground-state two degenarate orbitals of CH_3N and indicates that the Jahn−Teller effect is not evident as is shown in Table 5a.

Conclusions

High-level ab initio calculations were performed to study and characterize some low-lying electronic states of CH_3N and CH_3CH_2N and their positive and negative ions using 6-311++g(3df,3pd) basis sets and CASPT2//CASSCF methods.

The CASSCF geometry for the $1^3A''$ (R(C−N) = 1.446 Å and ∠HCH = 108.39°) state of CH_3N is compared with the experimental geometry for the $\tilde{X}^3A_2$ (R(C−N) = 1.411 Å and ∠HCH = 106.7°) state. We realize that the experimental geometry for the $1^3A''$ state of CH_3N was not accurately determined since the C−H bond length value was assumed to be 1.09 Å. The CASSCF/MCLR frequency calculations predict analogous values for the $1^3A''$ ground state of CH_3N compared with the experimental data. We predict the geometries and vibrational frequencies of several states of CH_3N and CH_3CH_2N. The Jahn−Teller effect is not evident except in the $^2A'$ and $^4A'$ states of CH_3N^+ and $CH_3CH_2N^+$.

The calculated transitions of CH_3N at 32 172 and 32 139 cm^{-1} are attributed to the $2^3A'' \rightarrow 1^3A''$ and $1^3A' \rightarrow 1^3A''$, respectively, which is in accordance with the $\tilde{A}^3E \rightarrow \tilde{X}^3A_2$ emission spectrum at T_0 = 31 817 cm^{-1} and is assigned to be $(ps)_H \rightarrow (sp)_\sigma$ in nature. For CH_3CH_2N, the transition energy is red shifted.

Theoretical studies for the ionization energies of CH_3N and CH_3CH_2N are compared with the experimental PES data. We predict a strong transition in the adiabatic excitation spectrum of CH_3N^+ at λ = 334 nm. We predict a weak transition in the adiabatic excitation spectrum of CH_3N^- at λ = 582 nm.

Acknowledgment. This work is supported by the Natural Science Foundation of China (20573042, 20333050, 20173021).

Supporting Information Available: Tables 9a and 9b giving Mulliken charges and basis function types for CH_3N and CH_3CH_2N and Figure 2 showing selected molecular orbitals of CH_3N. This material is available free of charge via the Internet at http://pubs.acs.org.

References and Notes

(1) Wentrup, C. *Reactive Molecules: The Neutral Reactive Intermediates in Organic Chemistry*; Wiley: New York, 1984; Chapter 4.
(2) Sadygov, R. G.; Yarkony, D. R. *J. Chem. Phys.* **1997**, *107*, 4994.
(3) Kurosaki, Y.; Takayanagi, T.; Sato, K.; Tsunashima, S. *J. Phys. Chem. A* **1998**, *102*, 254.
(4) Yarkony, D. R.; Schaefer, H. F., III; Rothemberg, S. *J. Am. Chem. Soc.* **1974**, *96*, 5974.
(5) Huber, K.; Herzberg. *Constants of Diatomic Molecules*; Van Nostrad: New York, 1979.
(6) Baronavski, A. P.; Miller, P. G.; Mcdonald, J. R. *Chem. Phys.* **1978**, *30*, 119.
(7) Foy, B. R.; Casassa, M. P.; Stephenson, J. C.; King, D. S. *J. Chem. Phys.* **1989**, *90*, 7037.
(8) Moore, C. B.; Pimentel, G. C.; Goldfarb, T. D. *J. Chem. Phys.* **1965**, *43*, 63.
(9) Dickens, J. E.; Irvine, W. M.; Devries, C. H. *Astrophys. J.* **1997**, *479*, 307.
(10) Carrick, P. G.; Engelking, P. C. *J. Chem. Phys.* **1984**, *81*, 1661.
(11) Chappell, E. L.; Engelking, P. C. *J. Chem. Phys.* **1988**, *89*, 6007.
(12) Ferrante, R. F. *J. Chem. Phys.* **1987**, *86*, 25.
(13) Carrick, P. G.; Brazier, C. R.; Bernath, P. F.; Engelking, P. C. *J. Am. Chem. Soc.* **1987**, *109*, 5100.
(14) Shang, H.; Yu, C.; Ying, L.; Zhao, X. *J. Chem. Phys.* **1995**, *103*, 4418.
(15) Shang, H.; Zhao, X. *Chem. Phys. Lett.* **1997**, *267*, 345.
(16) Demuynck, J.; D, Fox, J.; Yamaguchi, Y.; Schaefer, H. F., III. *J. Am. Chem. Soc.* **1980**, *102*, 6204.
(17) Nguyen, M. T. *Chem. Phys. Lett.* **1985**, *117*, 290.
(18) Rechards, C., Jr.; Meredith, C.; Kim, S.; Quelch, G. E.; Schaefer, H. F., III. *J. Chem. Phys.* **1994**, *100*, 481.
(19) Ferrante, R. F.; Erickson, S. L.; Peek, B. M. *J. Chem. Phys.* **1987**, *87*, 2421.
(20) Arenas, J. F.; Marcos, J. I.; Tocon, I. L.; Otero, J. C.; Soto, J. *J. Chem. Phys.* **2000**, *113*, 2282.
(21) Zeng, Y.; Sun, Q.; Meng, L.; Zheng, S.; Wang, D. *Chem. Phys. Lett.* **2004**, *390*, 362.
(22) Jing, W.; Zheng, S.; Xinjiang, Z.; Xiaojun, Y.; Maofa, G.; Dianxun, W. *Angew. Chem., Int. Ed.* **2001**, *40*, 3055.
(23) Yang, X.; Zheng, S.; Maofa, G.; Zheng, S.; Meng, L.; Wang, D. *ChemPhysChem* **2002**, *11*, 963.
(24) Travers, M. J.; Cowles, D. C.; Clifford, E. P.; Ellison, G. B. *J. Chem. Phys.* **1999**, *111*, 5349.
(25) Hou, X.-J.; Huang, M.-B. *Chem. Phys. Lett.* **2003**, *379*, 526.
(26) McLean, A. D.; Chandler, G. S. *J. Chem. Phys.* **1980**, *72*, 5639.
(27) Serrano-Andres, L.; Merchan, M.; Nebot-Gil, I.; Lindh, R.; Roos, B. O. *J. Chem. Phys.* **1993**, *98*, 3151.
(28) Andersson, K.; et al. *MOLCAS 5.4*; University of Lund: Lund, Sweden, 2002.
(29) Kemnitz, C. R.; Ellison, G. B.; Karney, W. L.; Borden, W. T. *J. Am. Chem. Soc.* **2000**, *122*, 1098.